

ULTRALUMINOUS X-RAY SOURCES POWERED BY RADIATIVELY EFFICIENT TWO-PHASED SUPER-EDDINGTON ACCRETION ONTO STELLAR MASS BLACK HOLES

ARISTOTLE SOCRATES^{1,2} AND SHANE W. DAVIS³

Draft version November 28, 2018

ABSTRACT

The radiation spectra of many of the brightest ultraluminous X-ray sources (ULXs) are dominated by a hard power law component, likely powered by a hot, optically thin corona that Comptonizes soft seed photons emitted from a cool, optically thick black hole accretion disk. Before its dissipation and subsequent conversion into coronal photon power, the randomized gravitational binding energy responsible for powering ULX phenomena must separate from the mass of its origin by a means other than, and quicker than, electron scattering-mediated radiative diffusion. Therefore, the release of accretion power in ULXs is not necessarily subject to Eddington-limited photon trapping, as long as it occurs in a corona.

Motivated by these basic considerations, we present a model of ULXs powered by geometrically thin accretion onto stellar mass black holes. In the region closest to the hole (region I), where the majority of the binding energy is released, cool thermal disk radiation is Comptonized by an adjacent corona covering the entire surface of the disk. The amount of reprocessed thermal emission in region I is quite small compared to the hard coronal output since the disk behaves as a near perfect reflector of X-rays, a result of the intense ionizing flux which leads to an extreme state of photo-ionization. If energy injection takes place within an optically thin corona, the conversion of binding energy into a wind is hampered by Compton drag and the wind's low optical depth. Furthermore, if the magnetic field geometry of the corona is primarily closed, then magnetic fields of modest strength can in principle, prevent the launching of a wind. In the outer regions (region II), where the albedo is somewhat lower, thermal emission resulting from a combination of viscous dissipation within the body of the disk and reprocessed coronal power is emitted at relatively low temperatures, due to the large surface area. Within the context of the current black hole X-ray binary paradigm, our ULX model may be viewed as an extension of the very high state observed in Galactic sources.

Subject headings: accretion, accretion disks – black hole physics – X-rays: binaries – X-rays: galaxies

1. OVERVIEW OF OBSERVATIONS, CURRENT INTERPRETATIONS, AND PLAN OF THIS WORK

Per detected photon, ultraluminous X-ray sources (ULXs) garner a disproportionate amount of attention. The reason for such relative popularity results from the two most common interpretations of their observed behavior: 1) super-Eddington luminosities resulting from accretion onto stellar mass black holes 2) sub-Eddington accretion onto intermediate mass black holes. Both explanations are problematic from a theoretical point of view. With respect to super-Eddington luminosities, it is not clear how a radiatively efficient flow can release binding energy at a rate above the Eddington limit in a steady-state manner. As for intermediate mass black holes, a well-established evolutionary path that accounts for their birth does not exist.

Below, we summarize some important observational features of ULXs and previous theoretical models of their behavior in hopes to motivate our own work.

1.1. *Observations*

We are primarily concerned with ULXs which display isotropic X-ray luminosities $L_X \gtrsim 10^{40} \text{ erg s}^{-1}$ – of order

10 times the Eddington limit for a $10M_\odot$ black hole. The radiation spectra of these sources measured by *Chandra* and *XMM* can be roughly fit by a power law with spectral index $\Gamma \sim 2$ (see Miller & Colbert 2004 for a comprehensive review). For highly studied ULX sources, fits to the data allow for the presence of a soft thermal component with $kT \sim 0.1 - 0.5 \text{ keV}$ in addition to a $\Gamma \sim 2$ power law. The presence of such an anomalously cool thermal component in many ULXs, along with the large inferred X-ray luminosity, provides the best argument for the presence of intermediate mass black holes. That is, large luminosities emitted thermally at relatively low temperatures necessarily requires a relatively large emitting area and therefore, more massive black holes.

Table 1 lists the salient observational features of highly studied ULXs, selected on the basis of their large luminosities as well as the ability of other workers to fit the data, in a statistically meaningfully way, with a two-component model consisting of a power law and soft multi-color disk black body. Clearly, the power law component in each individual source is a crucial component of the total X-ray power. To illustrate this point, Figure 1 provides best-fit theoretical spectra for two sources listed in Table 1. By extrapolating the power law component to 100 keV, the potential domination of the power law spectral component is further emphasized.

1.2. *Previous Interpretations*

¹ Department of Astrophysical Sciences, Princeton University, Peyton Hall-Ivy Lane, Princeton, NJ 08544; socrates@astro.princeton.edu

² Hubble Fellow

³ Department of Physics, University of California, Santa Barbara, CA 93106; swd@physics.ucsb.edu

TABLE 1
SPECTRAL PROPERTIES OF SELECTED ULXs

Source	Date	$k_B T_d$ (keV)	Γ	$F_{\text{pl}}/F_{\text{total}}$	L_X (10^{40} erg s $^{-1}$)	N_H (10^{21} cm $^{-2}$)	Reference
NGC 1313 X-1	2000 Oct 17	0.23 ± 0.02	1.76 ± 0.07	0.74 ^a	0.6 ± 0.1^a	3.1 ± 0.3	1
NGC 1313 X-2	2000 Oct 17	$0.16^{+0.16}_{-0.04}$	$2.3^{+0.2}_{-0.1}$	0.63 ^b	$0.66^{+0.18}_{-0.20} b$	3^{+3}_{-1}	2
M81 X-9	2002 Apr 10	$0.26^{+0.02}_{-0.05}$	1.73 ± 0.08	0.85 ^a	$1.1^{+0.3}_{-0.1} a$	2.3 ± 0.3	1
M81 X-9	2002 Apr 16	0.21 ± 0.04	1.86 ± 0.06	0.84 ^a	$1.3^{+0.3}_{-0.2} a$	2.9 ± 0.3	1
NGC 4038/4039 X-11	2002 Jan 8	0.15 ± 0.02	1.9 ± 0.2	0.61 ^a	$2.1^{+0.1}_{-1.1} a$	$3.0^{+0.8}_{-1.8}$	3
NGC 4038/4039 X-16	2002 Jan 8	0.19 ± 0.05	1.4 ± 0.2	0.33 ^a	$1.6^{+0.4}_{-1.0} a$	1.5 ± 1.0	3
NGC 4038/4039 X-44	2002 Jan 8	$0.15^{+0.02}_{-0.15}$	$2.2^{+0.1}_{-0.4}$	0.77 ^a	$1.0^{+1.3}_{-0.2} a$	$1.4^{+2.0}_{-0.4}$	3
NGC 4559 X-7	2003 May 27	0.148 ± 0.006	$2.23^{+0.05}_{-0.04}$	0.63 ^c	2.2 ^c	$5.1^{+1.4}_{-1.3}$	4
NGC 4559 X-7	2001 Jun 4	0.12 ± 0.006	1.8 ± 0.08	0.69 ^c	1.9 ^c	$3.6^{+0.9}_{-1.1}$	4
NGC 4559 X-7	2002 Mar 14	0.12 ± 0.01	2.13 ± 0.08	0.54 ^c	3.2 ^c	$5.7^{+0.9}_{-1.1}$	4
M74 X-1	2001 Oct 19	0.31 ± 0.05	$1.83^{+0.55}_{-0.58} e$	0.78 ^a	0.4 ^a	0.48	5
Holmberg II X-1	2002 Apr 10	$0.141^{+0.018}_{-0.015}$	$2.64^{+0.06}_{-0.06}$	0.83 ^d	2.0 ^a	$1.6^{+0.2}_{-0.1}$	6
Holmberg II X-1	2002 Apr 16	$0.128^{+0.022}_{-0.013}$	$2.40^{+0.07}_{-0.08}$	0.74 ^d	1.7 ^a	1.4 ± 0.3	6
Holmberg II X-1	2002 Sep 18	$0.120^{+0.022}_{-0.017}$	$2.89^{+0.07}_{-0.08}$	0.68 ^d	0.5 ^a	$1.4^{+0.5}_{-0.4}$	6
Holmberg II X-1	2004 Apr 15	0.20 ± 0.02	2.64 ± 0.03	0.91 ^d	1.2 ^d	$1.66^{+0.10}_{-0.09}$	7
NGC 5204 X-1	2003 Jan 6	0.21 ± 0.03	1.97 ± 0.07	0.82 ^{a,f}	0.44 ^a	$0.78^{+0.27}_{-0.17}$	8
NGC 5204 X-1	2003 Apr 25	$0.21^{+0.04}_{-0.03}$	$2.09^{+0.12}_{-0.13}$	0.69 ^{a,f}	0.55 ^a	$1.22^{+0.34}_{-0.29}$	8
M101 XMM-1 (P13/H19)	2002 Jun 4	$0.30^{+0.04}_{-0.06}$	$1.41^{+0.25}_{-0.18}$	0.74 ^a	0.27 ^a	$0.67^{+0.41}_{-0.19}$	9
NGC 7771 X-2	2002 June 21	$0.16^{+0.12}_{-0.03}$	$1.67^{+0.27}_{-0.26}$	0.80 ^a	$3.86^{+0.1}_{-3.21} a$	$3.18^{+4.49}_{-2.51}$	10

REFERENCES. — (1) Miller et al. (2004a); (2) Miller et al. (2003); (3) Miller et al. (2004b); (4) Cropper et al. 2004; (5) Krauss et al. 2005; (6) Dewangan et al. 2004; (7) Goad et al. 2005; (8) Roberts al. 2005; (9) Jenkins et al. 2004; (10) Jenkins et al. 2005

^aCalculated over the energy range 0.3-10 keV.

^bCalculated over the energy range 0.2-10 keV.

^cCalculated over the energy range 0.3-12 keV.

^dCalculated over the energy range 0.3-2 keV.

^eTheir definition of Γ is equal to our definition minus one

^fWe calculated the ratio based on parameters of their best-fit model.

Several models have been put forth to explain ULX phenomenon. For $L_X \gtrsim 10^{40}$ erg s $^{-1}$, accretion onto intermediate mass black holes (IMBHs) receives much attention. If interpreted as emission from an optically thick accretion disk extending to the inner-most stable circular orbit of the black hole, the temperature of the soft thermal component inferred from the spectra of these sources are consistent with black hole masses of $\sim 10^2 - 10^3 M_\odot$. However, the large fraction of non-thermal emission in these sources (see Table 1) brings into question the robustness of this interpretation. That is, the IMBH argument is straightforward only when the cool thermal component is associated with the majority of the bolometric luminosity, rather than a *sub-dominant* fraction of the gravitational power.

Alternatively, ULXs may result from accretion onto $\sim 10 M_\odot$ black holes. In this case, the emission must either be beamed so that the intrinsic energy release is less than that inferred (King 2001) or the Eddington limit must be exceeded. Begelman (2002) suggests that the non-linear development of the photon bubble instability (Gammie 1998; Blaes & Socrates 2003; Turner et al. 2005) might produce channels in the accretion flow, allowing the disk luminosity to exceed the Eddington limit since radiative trapping is overcome. In this work we propose an alternative scenario for generating steady state super-Eddington luminosities from stellar mass black holes, with the intent of reproducing the

hard, non-thermal emission that dominates the spectra of many bright ULXs.

1.3. Plan of this work

In the light of the rough observational guidelines outlined in §1.1 for ULXs, an accretion model describing ULX behavior must contain certain indispensable ingredients. Most importantly, the observed large fluxes should be released non-explosively. A good candidate is radiatively efficient accretion onto a compact object, whose birth and origin are well understood. Such an accretion flow must account for the large apparent coronal output while simultaneously accounting for the sub-dominant and relatively cool 0.1-0.5 keV thermal emission component.

In the next section we provide the framework in which the above observational constraints are satisfied. In §2.1 the central idea of this work is motivated and argued. That is, the release of accretion power resulting from a two-phased accretion flow is not bound by the Eddington limit since radiative diffusion, mediated by electron scattering, is not primarily responsible for the removal of randomized binding energy from the mass of its origin. The feasibility of confining coronal magnetic fields as well as the effects of Compton drag on the outgoing optically thin wind are discussed in §2.2 and §2.3, respectively. The formation of ULX spectra in terms of a corona+disk model is considered in §3 and we conclude in §4.

2. THE BASIC IDEA AND INITIAL ESTIMATES

Perhaps the most important assumption of one-zone models of accretion is that the randomized gravitational binding energy is dissipated locally with the mass of its origin. In the case of thin accretion disks, the gravitational power is transported vertically via radiative diffusion from the midplane of disk, where most of the mass resides. As a result, super-Eddington accretion rates do not proportionally lead to super-Eddington luminosities since the radial inflow time becomes short relative to the time it takes for a photon to escape from the disk midplane. That is, the photon trapping radius moves outward with accretion rate, negating the increase in available binding energy with a decrease in the overall radiative efficiency.

Another consequence of the local dissipation assumption is that the emergent radiation spectrum will be thermal and approach the black body limit. However, spectral components that probe the central engines of active galactic nuclei (AGN) and X-ray binaries (XRBs) indicate the presence of powerful non-thermal coronal emission accompanied by a soft quasi-thermal component. A common interpretation of AGN and XRB spectra is two-phased accretion onto a black hole (Haardt & Maraschi 1991, 1993, hereafter HM91, HM93; Svennsson & Zdziarski 1994, hereafter SZ94). In these models, a fraction f of the gravitational energy release is assumed to dissipate in a hot diffuse corona, above the main body of the disk, away from the majority of the accreted mass. It is typically thought that the viscous stress, assumed to be magnetic in nature (Balbus & Hawley 1991, hereafter BH91), transports angular momentum and initially randomizes the gravitational binding energy near the midplane. The magnetized fluid elements, which are buoyant

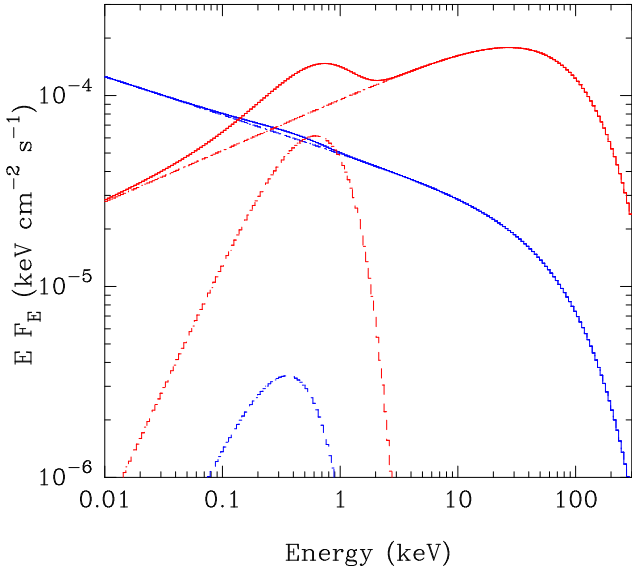


FIG. 1.— The best fit MCD + power-law model spectra are plotted for NGC 4038/4039 X-44 (blue) and M89 X-9 (2002 Apr 10; red). The curves represent the flux in the unabsorbed total model (solid), MCD component (dashed), and power-law component (dot-dashed) for the parameters listed in Table 1. Note that the models were fit with a power-law component over the 0.3-10 keV bands, but we have extrapolated the models assuming 100 keV cut-off to the power-law for the purpose of illustration. We have also rescaled the overall flux of M89 X-9 for illustrative purposes as well.

with respect to their surroundings, dissipate – perhaps through magnetic reconnection or shocks – above the disk where the reconnection time and Mach number are large.

For large values of f , often necessary to fit XRB and AGN data, the non-local dissipation of binding energy can have profound consequences on the disk structure as well as the net radiative efficiency. By introducing a mechanism of energy transfer other than radiative diffusion, the relevance of the Eddington limit is diminished (but not eliminated entirely). Below, we qualitatively discuss why super-Eddington luminosities may result for two-phased accretion onto a black hole.

2.1. Altered disk structure and trapping radius

Following SZ94, we assume that all of the accretion takes place in the main body of the disk. Since we are interested in explaining ULX behavior with stellar mass black holes, we restrict our discussion to accretion rates above the Eddington limit for a $3\text{-}20 M_{\odot}$ black hole, implying a radiation pressure dominated disk.

The difference in structure between a standard thin disk and that of a disk + corona is due the condition of radiative equilibrium

$$F_d = \sigma T_{eff}^4 = (1-f) Q = (1-f) \frac{3}{8\pi} \frac{GM\dot{M}}{R^3} \mathcal{D} \quad (1)$$

where Q is the viscous dissipation rate per unit area. All changes to disk quantities due to coronal dissipation depends on $(1-f)$ and for reference, their values (as well as definitions of the various disk quantities) with respect to standard thin disk scalings are given in Appendix A. Most notably, when compared to its classic one-zone counterpart, the disk scale height H_d decreases by a factor $(1-f)$ and therefore, the cool disk remains thin as long as an increase in \dot{m} is proportionately matched by an increase in f . Furthermore, decreasing the internal dissipation increases the disk midplane density increases by a factor $(1-f)^{-3}$. This has the important consequence that now, the radial inflow velocity becomes

$$v_R = \frac{\dot{M}}{4\pi RH_d \rho_d} = v_{0R} (1-f)^2 \propto \dot{M}^2 (1-f)^2 \quad (2)$$

where v_{0R} is the classic thin disk value (SS73). As long as increasing \dot{m} is matched by an increase in f , then v_R remains fixed, implying a reduction in the level of radiative trapping. To quantify this statement even further, we define the trapping radius R_{tr} , defined as the radius at which the radial inflow time is equal to the vertical diffusion time,

$$R_{tr} \sim \frac{1}{2^{1/2}} R_g (1-f)^{1/2} \dot{m}. \quad (3)$$

As expected, an increase in \dot{m} is matched by an increase in R_{tr} , directly leading to a decrease in radiative efficiency. For $f \sim 0$ at the Eddington accretion rate, the trapping radius $R_{tr} \sim 10R_g$ for a Schwarzschild hole. This implies that thin disk accretion cannot maintain its radiative efficiency beyond the Eddington accretion rate if the release of binding energy is governed by electron scattering-mediated radiative diffusion. However, for large values of f the binding energy of the gas is removed from large to small optical depths by a mechanism other than radiative diffusion, perhaps magnetic

buoyancy or waves. In this case, the modified radial inflow time R/v_R must be compared to the characteristic timescale of say, buoyant transport.

Without a coherent theory of relativistic accretion disk turbulence, it is difficult to estimate what the characteristic speed of magnetized buoyant transport v_B will be. A good guess for the upper limit of v_B is the sound speed of the disk at the midplane c_s . Let us define an inward advection time $\tau_{adv} \equiv R/v_R$ and a timescale for upward buoyant transport $\tau_B \equiv H_d/c_s$. As long as the ratio $\tau_{adv}/\tau_B > 1$, the accretion power of the flow stands a chance of escaping before being consumed by the black hole. In terms of disk quantities, we have

$$\frac{\tau_{adv}}{\tau_B} \lesssim \frac{r^{1/2}\tau_d}{\dot{m}} \simeq \frac{r^2}{\alpha \dot{m}^2 (1-f)^2} \quad (4)$$

If we (somewhat arbitrarily) take α to be ~ 0.1 , then the above ratio assumes a minimum value of $\tau_{adv}/\tau_B \sim 5$ at $r \sim 12$, the radius of maximum light, for an accretion rate rate of $\dot{m} = 175$ – ten times the Eddington rate – for a choice of $(1-f) \sim 0.1$. Therefore, the efficiency of the disk remains unchanged as long as an increase in the accretion rate \dot{m} is proportionately matched by a decrease in $(1-f)$. Even if the rate at which randomized gravitational binding energy leaks upwards decreases by a factor of ~ 5 , the disk may maintain its radiative efficiency for accretion rates of order ~ 10 times the Eddington rate.

2.2. Magnetic field requirements

Any viable accretion model that steadily generates super-Eddington luminosities must fulfill two requirements. First, the accretion flow must remove its randomized binding energy before being advected into the hole in order to maintain a large radiative efficiency. Furthermore, the majority of that binding energy must be converted into radiation rather than a mechanical outflow. The central point of this paper, encapsulated by eq. (4), addresses the first requirement. That is, magnetic buoyancy is an ideal mechanism for the non-dissipative removal of binding energy from the bulk of the flow. Addressing the second requirement is conceptually more difficult and again, we appeal to the existence of magnetic fields.

Irrespective of the geometry of the emitting surface, a super-Eddington radiation flux produces an outward opposing acceleration that is larger than the attractive inward acceleration provided by gravity (see e.g., Abramowicz et al. 1980). Therefore, an additional force or stress is required in order for our super-Eddington accretion model to maintain its radiative efficiency. Begelman (2002) suggests that strong magnetic fields might prevent surface regions of low optical depth from being blown off by a super-Eddington flux generated near the disk midplane. Furthermore, several authors have noted that accretion flows which liberate a sizable fraction of their binding energy in a Comptonizing corona inevitably require modest magnetic fields in order to mitigate the escape of pairs by the act of confinement (Svensson 1984; Zdziarski 1985; White & Lightman 1989). We examine a similar scenario in the context of the super-Eddington flux arising from energy injection in an optically thin corona. If indeed the confinement is provided for by magnetic fields, then there are some straightforward constraints regarding its topology and strength.

Charged particles are free to move along magnetic field lines. As long as the field lines are anchored in the disk, the supposed site of their generation, their magnetic tension is capable of confining fluid elements. Numerical simulations of stratified accretion flows indicate that the coronal field geometry is primarily closed and toroidal (Miller & Stone 2000; Hirose et al. 2004). However, it is not clear whether or not field lines are anchored deep in the disk. To gain an order of magnitude estimate of the acceleration a confining magnetic field can impart to a electrically conducting coronal fluid element, we define g_M to be a characteristic magnetic acceleration as

$$g_M \sim \frac{v_A^2}{H_c} \sim 10^{13} \left(\frac{v_A}{0.1c} \right)^2 \left(\frac{R_g}{H_c} \right) \left(\frac{10}{m} \right) \text{ cm s}^{-2}, \quad (5)$$

which should be compared to the magnitude of the gravitational acceleration

$$g \sim 10^{15} \left(\frac{10}{m} \right) \left(\frac{H_c}{R_g} \right) r^{-3} \frac{\mathcal{C}}{\mathcal{B}} \text{ cm s}^{-2}, \quad (6)$$

and the radiative acceleration

$$g_{rad} = \frac{\kappa_{es}}{c} F_d \sim 2 \times 10^{17} \left(\frac{10}{m} \right) \left(\frac{\dot{m}}{175} \right) r^{-3} \frac{\mathcal{D}}{\mathcal{B}}, \quad (7)$$

which has a maximum value of $g_{rad} \sim 2 \times 10^{13}$ for $\dot{m} = 175$ at $r \sim 12$. Note, \dot{m} is the accretion rate scaled to the Eddington rate $\dot{M}_{Edd} = 4\pi GMm_p/(c\sigma_T)$ and m is the black hole mass in units of M_\odot . If the radiative force in the corona is balanced by gradients in the magnetic field, then the ratio $g_M/g_{rad} \geq 1$ and the quantity g_{rad}/g is approximately the factor by which the Eddington limit is surpassed. If we assume that H_c and R scale in proportion to the mass of the hole, then like g , the characteristic magnetic and radiative acceleration g_M and g_{rad} are $\propto M_{BH}^{-1}$ and therefore in principle, similar Eddington ratios can be achieved for supermassive black holes.

The magnetic field strength or pressure in the corona can be constrained as well. First, the magnetic pressure of the corona $P_{m,c} \sim B_c^2/8\pi$ must be at least comparable to the coronal pressure. The other requirement is that the coronal magnetic pressure can not exceed the magnetic pressure at the disk midplane. Following the scalings of SZ94, the required coronal field strength is given by equating $P_{m,c}$ to $P_{rad,c}$ (see Appendix A), which yields

$$B_c \gtrsim 2.4 \times 10^8 \dot{m}^{1/2} \Lambda^{1/2} r^{-3/2} \left(\frac{\mathcal{D}}{\mathcal{B}} \right)^{1/2} \text{ G} \quad (8)$$

for $f \sim 1$. By assuming a magnetic origin for the accretion torque, an estimate of the magnetic field strength in the disk midplane is obtained by setting $P_{m,d} \sim \tau_{R\phi} \sim \alpha P_d$, giving us

$$B_d \simeq 1.6 \times 10^8 (1-f)^{-1/2} r^{-3/4} \left(\frac{\mathcal{C}}{\mathcal{A}} \right)^{1/2} \text{ G}. \quad (9)$$

For $\dot{m} = 175$, $f = 0.9$, and $\Lambda \sim 1$ at a radius of $r \sim 12$ the ratio $B_d/B_c \sim 3$, which is its lowest value. Thus it seems possible that if only a fraction of the dynamo-generated flux resides in the corona, the plasma there can be contained despite the upward force exerted upon it by the super-Eddington radiation field.

As a check of internal consistency, the coronal magnetic field given by eq. (8) must lead to an Alfvèn speed v_A

large enough to satisfy eq. (5). In order to evaluate v_A , knowledge of the coronal density is required. For a radiation pressure dominated corona, a characteristic density is roughly given in Appendix A, leading to an Alfvén speed of $v_A \sim c$ for the choice of disk and coronal parameters previously mentioned.

2.2.1. Hierarchy of stresses: Or, why coronae are essential for super-Eddington luminosities

Consider the following relevant thought experiment. Imagine injecting thermal energy into the Sun at a rate of $\sim 10^{39} \text{ erg s}^{-1}$, which is ~ 10 times its Eddington rate. Regardless of the depth at which this enormous deposition of energy takes place, the local pressure will similarly increase by a factor of ~ 10 . This can be understood by noting that the ratio of radiation to gas pressure P_{rad}/P_g is roughly a constant throughout the star and approximately equal to its Eddington factor such that $P_{\text{rad}}/P_g \sim L_{\odot}/L_{\text{Edd}}$.

If the injection takes place uniformly at a great depth near the core, then the resulting radiation stress is ~ 10 times larger than any other stress in the entire star. Thus, the bulk of the star has no choice other than to move outward and form a massive wind that carries away the injected energy. However, if the energy injection uniformly takes place at the surface and near the photosphere, then the situation can potentially be quite different. That is, a radiation pressure supplying a flux ~ 10 times the Eddington limit at the surface of the Sun is only $\sim 10^{-12}$ that of the gas pressure in the core. Hence, super-Eddington energy injection at the surface does not appreciably change the structure of the star. If the stresses within the star re-arrange themselves only slightly, then a super-Eddington flux due to energy injection at the surface can easily be confined as to stifle the production of a non-radiative super-Eddington wind. To further clarify this point, take the example of a sunspot, whose magnetic stresses are supposedly generated by highly subsonic (and highly sub-virial) turbulent and shearing motions at the base of the solar convection zone. For typical sunspot field strengths \sim a few $\times 10^3$ G, closed field lines at the photosphere could in principle, confine matter that is accelerated by radiation pressure of order ~ 10 times Eddington. Despite the fact that only an infinitesimal amount of the Sun's internal energy resides in its convection zone, subsonic motions in these regions may lead to stresses large enough to contain regions of the photosphere experiencing a super-Eddington radiation pressure.

The situation described in the previous section with respect to ULXs powered by super-Eddington accretion disks is quite similar to the solar thought experiment outlined above. Even for super-Eddington luminosities, the ratio of coronal to midplane pressure P_c/P_d is quite small. In the disk case, the magnetic accretion stress αP_d originates from motions that are subsonic in the midplane by a different mechanism than, but analogous to, the generation of field loops in the shear layer at the base of the solar convection zone. The arguments surrounding eqs. (8) and (9) indicate that if even a small fraction of the magnetic energy leaks into photosphere, magnetic confinement is a plausible mechanism for the suppression of a super-Eddington wind.

2.3. Compton-driven wind

In the absence of closed magnetic field lines, it is commonly thought that the majority of the gravitational power for a super-Eddington accretion flow either is advected into the black hole or is converted into mechanical energy that drives an outflow. In this two-phased accretion model, it is unlikely that a significant amount of the binding energy is advected into the hole for sufficiently large values of f , the fraction of power released in the corona. Therefore, most of the radiative luminosity would be expected to be converted into the kinetic power of the outflow. However, this conclusion follows from the assumption that the majority of the energy injection takes place beneath the photosphere.

The properties of continuum driven winds follow from conservation of momentum (Lamers & Cassineli 1999)

$$\rho v \frac{dv}{dR} + \frac{dP_g}{dR} + \rho \frac{GM}{R^2} = \frac{n_p \sigma T}{c} \frac{L}{4\pi R^2} \left(1 + 2 \frac{n_+}{n_p} \right) \quad (10)$$

and mass

$$\dot{M} = 4\pi R^2 \rho v. \quad (11)$$

Here, n_p is the number density of the ions and n_+ is the number density of pairs. For the sake of simplicity, we have assumed spherical symmetry. Since we are considering super-Eddington luminosities, the forces due to gravity and gas pressure can be neglected outside the sonic point. Integrating over space, eq. (10) then becomes

$$\dot{M} v_{\infty} \simeq \tau_p \frac{L}{c} \left(1 + 2 \frac{n_+}{n_p} \right), \quad (12)$$

where τ_p and v_{∞} are the plasma optical depth and outflow velocity at infinity, respectively. Note that the ratio n_+/n_p is approximated as constant. The above expressions are accurate for non-relativistic velocities. Due to the large radiative acceleration, a relativistic outflow seems inevitable. However, Compton drag limits the Lorentz factor Γ_L to moderate values, such that $\Gamma_L \gtrsim 1$ (Madau & Thompson 2000).

For $v_{\infty} \sim c$, the kinetic luminosity in the wind L_w is simply

$$L_w \sim \tau_p L \left(1 + 2 \frac{n_+}{n_p} \right). \quad (13)$$

Thus, the kinetic power resulting from super-Eddington energy injection is directly proportional to the total plasma + pair scattering optical depth and in principle, may be significantly smaller than the photon luminosity. These arguments are simple. In order to truly quantify the rate of loss of mechanical energy, the spatial distribution of energy injection must be specified, potentially allowing for a detailed calculation of the coronal structure, pair equilibrium, and resulting spectrum.

3. CORONAL STRUCTURE AND ULX SPECTRA

The radiation spectra of high luminosity ULXs are often dominated by a relatively flat $\Gamma \sim 2$ power law. Also, the fractional thermal emission, responsible for $\sim \frac{1}{3}$ to $\frac{1}{10}$ of the luminosity, is typically modeled by a black body or multi-temperature disk black body with a characteristic temperature of 0.1-0.5 keV. Along with producing

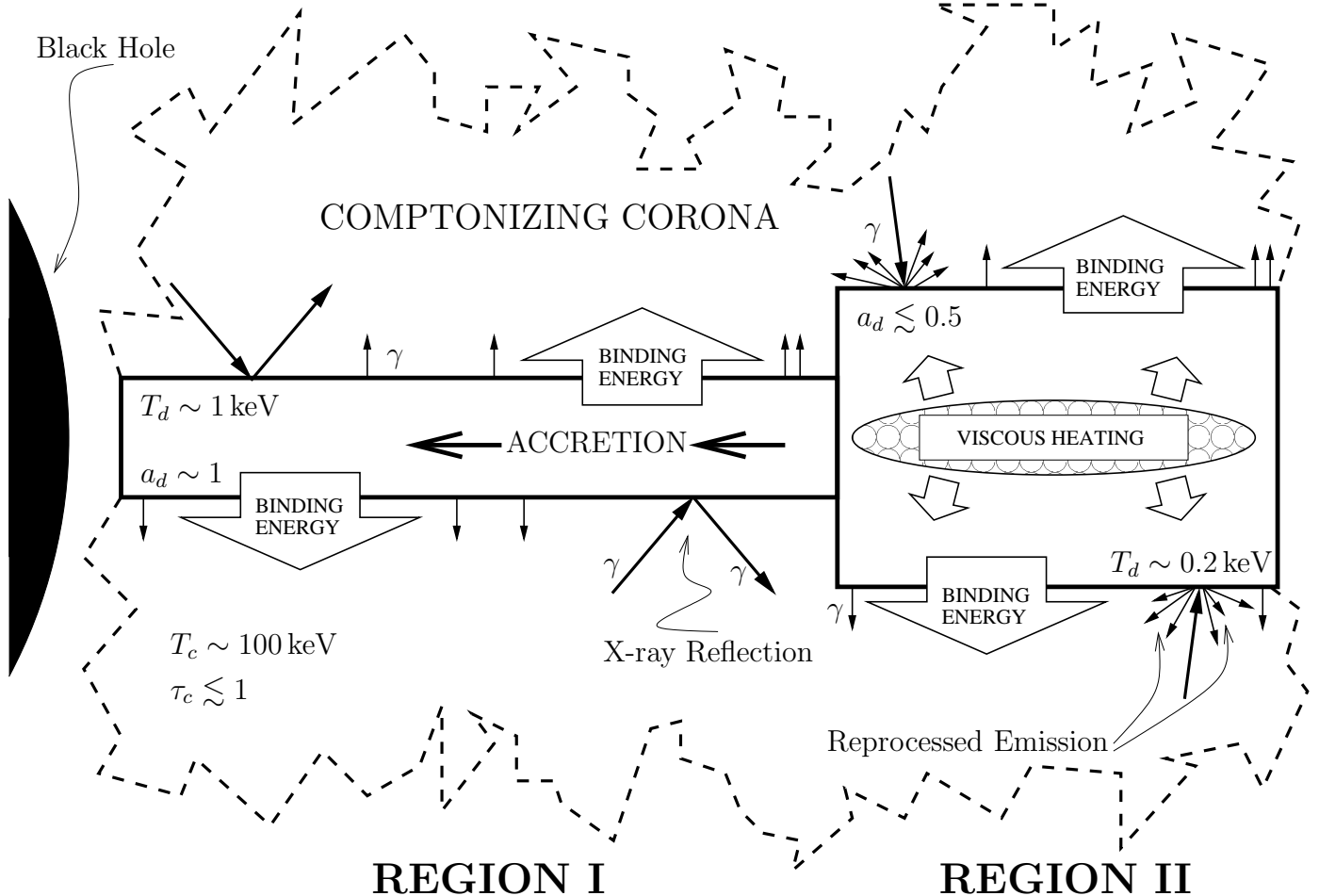


FIG. 2.— Sketch of our stellar mass black hole ULX accretion model. In both Regions I and II, gravitational binding energy is removed from the disk in the vertical direction before it is converted into heat. However, accretion power may dissipate locally in Region II without being advected into the hole. The majority of the gravitational power is released in Region I primarily in the form of hard Comptonized photons. Throughout the flow, cool photons from the optically thick disk are Comptonized in the surrounding hot diffuse corona. Hard X-ray photons incident upon the disk are nearly perfectly reflected in Region I while in Region II, they are photo-electrically absorbed by the disk. In the corona, the production of an energetically dominant super-Eddington wind is hindered by the presence of confining magnetic fields, a low optical depth, and the effects of Compton drag. Note that this figure is not to scale.

a luminosity of $\sim 10^{40} - 10^{41} \text{ erg s}^{-1}$, these two observational constraints must be reproduced by an accretion flow spectral model that describes ULX behavior.

Our model consists of a two-phased accretion flow divided into two distinct geometrically thin regions (see Figure 2). The inner portion of the disk, or region I, is responsible for liberating the majority of the system's gravitational binding energy, while the outer portion, region II, powers the sub-dominant thermal spectral component.

In region I, we adopt the slab geometry for the disk+corona i.e., the simplest configuration possible. In order to reproduce the spectra of luminous ULXs, region I cannot be a prodigious site of soft thermal photon power. Therefore, the emergent spectra from the region of deepest gravitational potential must resemble a $\Gamma \sim 2$ Comptonized power law with only a small fraction of the luminosity in the form of thermal emission such that ratio of hard coronal to soft power $L_c/L_s \sim 10$ in region I.

As described in the previous section, if randomized

binding energy is deposited in a corona in excess of the Eddington rate, hydrostatic balance cannot be achieved unless forces that are non-gravitational in nature, such as magnetic stresses, are present. In the absence of magnetic fields, the corona becomes geometrically thick and a wind develops. Calculating the structure of the corona by accurately including the relevant processes that accompany magnetic field generation and transport, non-equilibrium radiation physics, and winds is an impossibly difficult problem, with no clear way as to how to proceed. However, some simplification is achieved by realizing that Comptonization of ambient soft photons must be the radiative mechanism which mediates the release of energy in the corona. That is, relatively few physical parameters, such as optical depth and temperature, are required to reproduce the observed spectral components for a given coronal geometry. Though such an approach lacks almost any sense of predictive power, it provides a rough outline as to what the flow geometry and energetics might be.

In what follows, we briefly discuss the composite phys-

ical requirements of the accretion flow necessary to reproduce the observed spectra.

3.1. Spectral index, coronal temperature, and optical depth of the inner region

An almost universal feature of the spectral energy distributions (SEDs) of the relativistic accretion flows that power active galactic nuclei (AGN) and XRBs is a predominantly flat broadband X-ray power law which results from thermal Comptonization of hot coronal electrons. In AGN and black hole XRBs in the low/hard state, the spectral index $\Gamma \lesssim 2$, with greater variation seen in black hole XRBs.

In the case of low/hard state spectra of galactic black hole candidates such as Cyg X-1, both the local and disk-integrated values of $L_c/L_s \gg 1$. The most popular disk+corona geometry that is invoked to explain these sources is a truncated disk + hot inner spherical corona model (Poutanen, Krolik, & Ryde 1997; Esin et al. 1998). The inner hot regions are thought to resemble the ADAF/CDAF accretion models that are thought spontaneously occur at low accretion rates (Narayan & Yi 1995; Quataert & Gruzinov 1999). However, there are other explanations for the low/hard state that cannot be ruled out and both involve altering the patchy corona model of HMG93 by reducing the soft reprocessed disk emission. If the overwhelming majority of the flow's gravitational power is liberated in relatively small active coronal regions, then the ionizing flux incident upon the disk will be so large that the atomic X-ray absorptivity of the disk becomes vanishingly small and disk acts almost as a perfect reflector (Ross & Fabian 1993; Ross, Fabian, & Young 1999; Ballantyne, Ross, & Fabian 2001). Another mechanism that reduces reprocessed disk emission in the patchy corona model is outward vertical motion of the active regions at sub-relativistic velocities (Beloborodov 1999).

In region I of our ULX model, the local and disk-integrated value of $L_c/L_s \gg 1$ as in the case of black hole XRBs in the low/hard state. For a spectral index $\Gamma \sim 2$, equal photon power is emitted at all photon energies bounded by the input seed photon energy and the coronal electron temperature. Therefore, the majority of the disk photons interact with the corona only a few times, if any, and the relatively few photons that stay in the corona the longest carry away with them most of the radiated power. The likelihood for a photon to escape the corona, which varies inversely with the optical depth τ , is appropriately balanced by the average photon energy shift per scattering $\Delta E/E \sim 4k_B T_c/m_e c^2$ in order to reproduce a given spectral index Γ (see e.g., Fermi 1949 within the context of cosmic ray acceleration in the interstellar medium). Thus, if the $k_B T_e \sim 100$ keV, then only $\frac{1}{100}$ of the input photons would have to leave the system at that energy for a soft seed photon energy of ~ 1 keV and an outgoing spectral index $\Gamma \sim 2$. Such harmony can be achieved for $\tau \sim 1$ since $\Delta E/E \lesssim 1$ if $k_B T_e \sim 100$ keV. That is, a $\Gamma \sim 2$ Comptonized spectrum is viable only when the propensity of escape per scatter is proportionally countered by a gain in energy for every scattering event.

For flat $\Gamma \sim 2$ Comptonized spectra, the amplification L_c/L_s can be estimated by calculating the number of scattering orders N_s required to fill out the Comptonized

power law, since the location of each scattering order in the SED carries equal amounts of energy as the soft input. By choosing soft seed photon energies of order ~ 1 keV, roughly an Eddington's worth of power is emitted from the cold optically thick disk. From the argument above, $\Gamma \sim 2$ for coronal temperatures of order ~ 100 keV and an optical depth ~ 1 . For these parameters, we obtain $N_s \sim L_c/L_s \lesssim 10$. Thus, an input soft seed X-ray source typical for optically thick Eddington-limited accretion onto $10M_\odot$ black hole is amplified up to ~ 10 times its intrinsic thermal power if there is an adjoining corona with $T_e \sim 100$ keV and $\tau \sim 1$ covering the entire disk.

The somewhat prosaic arguments given above are in rough agreement with detailed Comptonization calculations of other authors (Pietrini and Krolik 1995; Stern et al. 1996). For example, Pietrini and Krolik (1995) deduced a scaling relationship between T_e , τ , L_c/L_s , and Γ that reproduce the desired spectral properties of our ULX coronal model. Similar to the low/hard state of black hole XRBs, our ULX model requires a low level of soft photon input. We cannot appeal to a truncated disk + ADAF/CDAF scenario because large accretion rates and high radiative efficiencies are necessary for ULXs. In order to reduce the amount of reprocessed thermal power, the albedo of the disk must approach unity due to the intense super-Eddington ionizing flux. In what follows, we discuss the validity of this assertion.

3.2. Albedo

In order to reproduce spectra dominated by a Comptonized power law in the slab geometry, the Comptonized photons incident upon the disk must avoid photo-electric absorption. If a significant fraction of the hard X-ray flux is absorbed by the disk, the reprocessed thermal emission can in principle be comparable to the local X-ray flux such that $L_c/L_s \sim 1$ in the slab geometry (Haardt & Maraschi 1991). Thus, either the disk albedo must approach unity as a result of photo-ionization (Ross & Fabian 1993) or the coronal electrons flow away from the disk at sub-relativistic to relativistic velocities (Beloborodov 1999).

In a super-Eddington model of ULXs, the ionizing coronal flux is intense in comparison to say, ionizing disk models of black hole XRBs in the low/hard state. An increase in disk albedo implies a change in the disk's role from that of an absorber and re-emitter to a reflecting X-ray mirror. If the disk albedo a_d approaches its limiting value such that $a_d = 1$, nearly all of the metal ions in surface of the disk must be fully ionized.

In Appendix B a_d is shown to closely approach unity near the inner-edge of the disk for $\dot{m} = 175$ while sharply dropping off at larger radii. By $r \sim 60$, outside of which $1/5$ of the gravitational power is released, $a_d \sim 1/2$. Therefore, one expects a significant amount, at least compared to the Eddington limit, of thermal emission to be emitted from ULX flows, despite the majority of the flow's gravitational power being released via Comptonization.

Eq. (B5) raises an interesting point. For accretion disks that power AGN, the abundant CNO metals are not fully ionized since the thermal disk temperatures are significantly lower. As a result, $A_Z \sim 10^{-2} - 10^{-3}$, implying that the disk cannot act as a perfect reflector and the

spectra will be different than the XRB case in that the reprocessed thermal spectral component is more likely to be comparable in magnitude to the Comptonized power law.

3.3. Thermal component

The inferred thermal component of bright ULXs are often cited as the most compelling evidence for the existence of intermediate mass black holes due to their relatively low temperatures. Roughly speaking, the most luminous sources can be fit just as well with a simple power law rather than a sub-dominant disk + dominant power law component. Therefore, explaining the physical processes responsible for the inferred soft thermal component is not central to our understanding of ULXs. Nevertheless, we describe the manner in which soft thermal emission may emerge from our ULX model.

In our model, thermal disk emission primarily originates from region II. Take the example of a $10M_{\odot}$ black hole accretion flow which resembles our ULX model accreting at 10 times the Eddington rate \dot{m}_{Edd} . For a non-rotating hole, the brightest region of the flow is located at $r \sim 12$ and since gravitational power falls off as $\propto r^{-1}$, roughly 90% of the accretion power is liberated within $r \sim 120$. Assume that this luminous inner portion of the flow constitutes region I. Outside this radius in region II, further assume that the dissipation and release of gravitational binding energy proceeds in the classical SS73 sense such that an Eddington's worth of gravitational power is emitted there as a result of viscous dissipation. In this case, the disk remains thin at $r \sim 120$ such that $H/R \lesssim 1$, the diffusion time is short compared to the inflow time, and the radiation spectra is roughly thermal. Compared to a disk with $\dot{m} = \dot{m}_{Edd}$ around the same black hole, the temperature of the thermal emission from region II in the ULX case is cooler due to its larger emitting surface. Typical inner-disk effective temperatures for an Eddington accretor around a $10M_{\odot}$ black hole are $k_B T_{eff} \sim 0.7$ keV, whereas the $\dot{m} = 10 \dot{m}_{Edd}$ ULX model radiates an equal amount of power at a lower temperature of $\sim 0.2 - 0.3$ keV.

An energetically dominant corona is required in order to generate more than an Eddington's worth of thermal power from region II in order to avoid the trapping and thickness problem. Therefore, super-Eddington values of thermal power must result from the reprocessing of coronal photons inside the trapping radius. If we increase the accretion rate to $50 \dot{m}_{Edd}$, then for the same emitting area for region II discussed above, ~ 5 times an Eddington's worth of thermal power will be emitted at a temperature of $\sim 0.4 - 0.5$ keV outside of $r \sim 120$. Evidently, our ULX model possesses the ability to produce over an Eddington's worth of thermal power for a $10M_{\odot}$ black hole at relatively low temperatures in what we have termed region II.

To mitigate the radiative inefficiencies due to the production of a powerful wind, which inevitably accompanies super-Eddington thermal fluxes, region II's corona must possess and ordered, predominantly azimuthal magnetic field. By use of eqs. (8) and (9), we see that the required coronal field strength B_c in region II is small compared to value of the field in the midplane such that $B_c/B_d \lesssim \frac{1}{10}$ for sufficiently large values of f .

4. DISCUSSION AND SUMMARY

Many bright ULXs exhibit power-law emission with hard $\Gamma \lesssim 2$ spectral indexes. In fact, recent *Chandra* survey data indicates that ULXs on average have $\Gamma \simeq 1.8$ with significant scatter, but independent of luminosity (Swartz et al. 2004). If ULXs are simply scaled up versions of Galactic black hole XRBs, then their $\Gamma \lesssim 2$ power-laws are consistent with the low/hard state spectra of Galactic sources (Remillard & McClintock 2003). For this scenario, the accretion flow is expected to be sub-Eddington such that $L_X \sim 10^{-2} L_{edd}$ (e.g. Maccarone 2003), implying black hole masses $\gtrsim 10^4 M_{\odot}$. In the ADAF/CDAF model of the hard state, the thermal emission is produced by a truncated disk at relatively large radii and correspondingly low temperatures. If we adopt this picture for ULXs, then the temperature of the truncated disk component would be a factor of 3-7 times lower than the ~ 0.1 keV truncated disk temperature found in Galactic black hole XRBs such as Cyg X-1 (Gierlinski et al. 1997; Poutanen, Krolik, & Ryde 1997). As a result, the thermal components near ~ 0.1 keV which are inferred from fits to some bright ULXs would not be produced in the truncated disk model.

Thus, an explanation of the soft thermal component inferred from bright ULX spectra requires a disk + corona geometry that is different from the above picture for Galactic XRBs, whether or not the central object is an IMBH. If ULXs are indeed powered by an IMBH ADAF/CDAF-type accretion flow, then the soft spectral component must come from another source such as diffuse nebular emission. In any case, for hard $\Gamma \lesssim 2$ power-laws, the soft component of ULXs cannot be utilized to deduce the mass of the black hole in a straightforward manner, unless the overall accretion geometry is markedly different from that of Galactic XRBs.

Our accretion model is primarily motivated by the fact that many bright ULXs are dominated by hard non-thermal photon power. This strongly suggests that radiative diffusion is not responsible for transporting the majority of the gravitational binding energy out of the accretion flow. Photon trapping, a mechanism which caps the luminosity of standard thin/slim disks, need not limit the flow's output to the Eddington value. For super-Eddington energy injection rates, the outward radiative acceleration outstrips the local gravitational acceleration. If reasonably strong magnetic stresses are present in the corona, the generation of a continuum-driven wind is prevented as long as the coronal field line are closed and anchored in the disk. In the absence of confining magnetic fields, the resulting wind inefficiently converts photon energy into outflowing mechanical power due to the effects of Compton drag and a low optical depth. Therefore, the majority of the super-Eddington accretion power is not necessarily converted into mechanical energy and thus, the flow's radiative efficiency is left relatively untouched. In the corona, randomized gravitational binding energy is converted into radiative power via Compton amplification of soft seed photons. As a result of the large downward ionizing flux deep in the gravitational potential, the disk's albedo is sufficiently high such that it behaves as a reflecting X-ray mirror and relatively little thermal emission emerges from the luminous inner regions. Further away from the black

hole a combination of reprocessed emission and viscous dissipation may produce roughly an Eddington's worth of photon power at low thermal energies since the emitting area is comparatively large.

Phenomenologically, our ULX model may be viewed as a natural extension of the commonly accepted picture of how Galactic black hole XRBs evolve with luminosity (e.g. Done & Gierliński 2004). For soft state XRBs, the ratio of coronal to soft power L_c/L_s increases with luminosity. In the “high state” $L_c/L_s \sim 0.1$ whereas in the “very high state,” typical values of $L_c/L_s \sim 1$. Furthermore, $L \sim 0.1 L_{Edd}$ in the high state while the luminosity of the very state approaches L_{Edd} and interestingly, $L_c/L_s \sim 10$ for ULXs with $L \sim 10 L_{Edd}$.

Of course, there are many theoretical uncertainties

uniquely haunting the ULX model presented in this work. In order to overcome the Eddington limit by a factor of $\simeq 10$, the fraction of binding energy released in the corona $f \simeq 0.9$ so that the bulk of the flow can expel its binding energy before being advected into the hole, while remaining geometrically thin. If magnetic fields are utilized as a confining mechanism in the corona, their strength, geometry, and stability must be considered in further detail. The net radiative efficiency of the flow hinges upon the assertion that the majority of the accretion power does not escape in a mechanical form. In order to verify this claim, the vertical structure of the corona resulting from the intense Comptonizing radiation field, must be be determined.

APPENDIX

A: DISK SCALINGS

In this appendix, we provide disk scalings relevant for the disk midplane following the work of SZ94. When the accretion rate is large we choose to ignore radial advection, an assertion that is justified as long as the fraction of the energy dissipated in the corona $f \simeq 1$ i.e., the regime relevant for ULX behavior.

In the radiation pressure dominated limit, the midplane disk quantities are given by

$$\frac{H_d}{R} = \frac{3}{2} \dot{m} r^{-1} (1-f) \frac{\mathcal{D}}{\mathcal{C}}, \quad (\text{A1})$$

$$\rho_d = \frac{8}{9} \frac{m_p}{\sigma_T R_g} \alpha^{-1} \dot{m}^{-2} r^{3/2} (1-f)^{-3} \frac{\mathcal{C}^2 \mathcal{B}}{\mathcal{D}^2 \mathcal{A}}, \quad (\text{A2})$$

$$\tau_d = \frac{4}{3} \alpha^{-1} \dot{m}^{-1} r^{3/2} (1-f)^{-2} \frac{\mathcal{C} \mathcal{B}}{\mathcal{D} \mathcal{A}}, \quad (\text{A3})$$

$$P_{rad,d} = P_d = \frac{2}{3} \frac{m_p c^2}{\sigma_T R_g} \alpha^{-1} r^{-3/2} (1-f)^{-1} \frac{\mathcal{C}}{\mathcal{A}}. \quad (\text{A4})$$

The factors $\mathcal{A} - \mathcal{D}$ enforce the no-torque inner boundary condition and take into account the effects of general relativity (Riffert and Herold 1995; Hubeny and Hubeny 1998). Note that the dimensionless cylindrical radius r is scaled to the gravitational, rather than Schwarzschild radius such that $r = R/R_g = R c^2/GM$. The four physical disk quantities above are determined by four conservation laws. Namely, conservation of mass, vertical momentum (hydrostatic balance), angular momentum, and energy (radiative equilibrium).

That is, we assume that it is possible for all of the angular momentum transport and accretion to take place in the body of the disk even if the overwhelming majority of the dissipation resulting from the action of accretion takes place in the corona. Thus, in order to constrain these quantities in the corona, we arbitrarily assume a value for the coronal optical depth τ_c . In the radiation pressure dominated limit, hydrostatic balance may be written as

$$\frac{\sigma_T F_d}{m_p c} = \frac{GM}{R^2} \frac{z}{R} \frac{\mathcal{C}}{\mathcal{B}} \quad (\text{A5})$$

where the left hand side is the upward radiative acceleration associated with a flux F_d , and the right hand side is the force of gravity in the thin disk limit. Defining H_c as the height above the midplane where $F_d = Q$ we find

$$\frac{H_c}{R} = \frac{3}{2} \dot{m} r^{-1} \frac{\mathcal{D}}{\mathcal{C}}. \quad (\text{A6})$$

Following SZ94, we estimate a coronal density from the scale height and optical depth $\tau_c = H_c \rho_c \sigma_T / m_p$.

Inserting eq. A6 for H_c in the radiation pressure dominated case yields

$$\rho_c = \frac{2}{3} \frac{m_p}{\sigma_T R_g} \dot{m}^{-1} \tau_c \frac{\mathcal{C}}{\mathcal{D}}, \quad (\text{A7})$$

For $\tau_c \lesssim 1$, the radiation pressure can be approximated as

$$P_{rad,c} \sim \Lambda \frac{Q}{c} = \frac{3\Lambda}{2} \frac{c^2 m_p}{\sigma_T R_g} \dot{m} r^{-3} \frac{\mathcal{D}}{\mathcal{B}} \quad (\text{A8})$$

where Λ is a factor of order unity which is determined by the angular dependence of the radiation field.

B: ESTIMATE OF DISK ALBEDO

The disk albedo a_d reaches large values when ϵ , the ratio of absorption to total opacity, is small. In order to keep the photo-electric absorption rate at a low value, the disk must be close to a fully ionized state, which is roughly determined by the density of the gas, number of ionizing photons, and recombination rate. A comparison with the results of other works is facilitated by the introduction of the “ionization parameter” ξ_I , given by

$$\xi_I \equiv \frac{4\pi F}{n_H} \simeq \frac{4\pi m_p f Q}{\beta \rho_d} \simeq 2 \times 10^6 \left(\frac{0.1}{\beta} \right) \left(\frac{\alpha}{0.1} \right) \left(\frac{\dot{m}}{175} \right)^3 \left(\frac{1-f}{0.9} \right)^3 \left(\frac{f}{0.9} \right) \left(\frac{r}{12} \right)^{-9/2} \text{ erg cm s}^{-1}. \quad (\text{B1})$$

Here, β parameterizes the density of the X-ray absorbing or reflecting region near the surface of the disk and is always chosen such that $\beta < 1$. We have eliminated the relevant relativistic and no-torque correction factors, which take on a value ~ 0.003 at $r \sim 12$. Detailed spectral and ionization calculations show that $a_d \sim 1$ when $\xi_I \sim 10^5$ (see Ballantyne 2002 for a concise review).

In the following, we motivate why $a_d \sim 1$ for $\xi_I \sim 10^5$ erg cm s $^{-1}$. For the sake of simplicity, we group all metals into a single hydrogenic species with abundance A_Z . This approximation is only valid when the absorber/reflector is close to being fully ionized and when the incident X-ray spectra is roughly described as having equal power across photon energy since different ions have different ionization potentials. With this, the expression that governs the balance between the number of hydrogenic and completely stripped ions is given by

$$n_i \int_{\nu_0}^{\infty} \frac{F_{\nu}}{h\nu} \sigma(\nu) d\nu = n_e n_{i+1} \alpha_R(T) \quad (\text{B2})$$

where n_i , n_{i+1} , n_e , F_{ν} , $\sigma(\nu)$, and $\alpha_R(T)$ is the number density of bound hydrogenic ions, number density of completely stripped ions, number density of free electrons, incident flux, absorption cross section, and recombination rate, respectively. By assuming a flat $\Gamma = 2$ spectral index for the ionizing continuum and that $\sigma(\nu) = \sigma_0 (\nu/\nu_0)^3$, an expression for the hydrogenic fraction χ_i reads

$$\chi_i^{-1} \equiv \frac{n_{i+1}}{n_i} = \frac{4\pi F_I}{n_H} \frac{\sigma_0}{16 h \nu_0 \alpha_R(T)} \frac{n_H}{n_e}. \quad (\text{B3})$$

Here $F_I \equiv \int_{\nu_0}^{\infty} F_{\nu}$ and if we further approximate that $F \sim F_I$ then by use of eq. (B4)

$$\chi_i^{-1} \sim 10^5 \left(\frac{\xi_I}{2 \times 10^6} \right), \quad (\text{B4})$$

for typical values of the micro-physical parameters i.e., $\sigma_0 \sim 10^{-18} \text{ cm}^2$, $h\nu_0 \sim 10 \text{ keV}$, and $\alpha_R(T) \sim 10^{-10} \text{ s}^{-1}$. Now, we are in a position to calculate ϵ the ratio of absorption to scattering opacity in terms of the fiducial metal abundance A_Z

$$\epsilon \sim \frac{\kappa_{abs}}{\kappa_{sc}} \sim \frac{\chi_i A_Z \sigma_0}{\sigma_T} \sim 5 \times 10^{-4} \left(\frac{A_Z}{5 \times 10^{-5}} \right) \left(\frac{2 \times 10^6}{\xi} \right). \quad (\text{B5})$$

Note that the value of A_Z corresponds to Fe at solar abundances. Due to the large disk temperatures in XRBs, the relatively abundant CNO metals are fully ionized. Finally, in order to calculate the a_d , the disk albedo, we make use of the two-stream approximation – an accurate approximation in the elastic limit for photon energies under 10 keV – for the disk surface layers (see e.g. HM93).

$$a_d \simeq \frac{1 - \epsilon^{1/2}}{1 + \epsilon^{1/2}} \simeq \frac{1 - 0.024}{1 + 0.024} \simeq 0.953 \quad (\text{B6})$$

for our choice of parameters at $r \sim 12$.

We thank O. Blaes, R. Kulsrud, B. Pacyński, J. Ostriker, E. Ramirez-Ruiz, J. Stone and D. Uzdensky for helpful conversations. SWD thanks the Institute for Advanced Study, where a portion of this work was completed, for its hospitality. AS acknowledges support of a Hubble Fellowship administered by the Space Telescope Science Institute.

REFERENCES

Abramowicz, M.A., Calvani, M., & Nobili, L. 1980, ApJ, 242, 772
 Balbus, S.A., & Hawley, J.F. 1991, ApJ, 376, 214
 Balbus, S.A. & Hawley, J.F. 1998, RvMP, 70, 1
 Ballantyne, D.R., Ross, R.R., & Fabian, A.C. 2001, MNRAS, 327, 10
 Ballantyne, D.R., Ross, R.R., & Fabian, A.C. 2002 in Workshop on X-ray Spectroscopy of AGN with Chandra and XMM-Newton, MPE Report 279, p. 73, astro-ph/0204260
 Begelman, M.C. 2002, ApJ, 568L, 97
 Beloborodov, A.M. 1999, ApJ, 510L, 123
 Cropper, M. et al. 2004, MNRAS, 349, 39
 Dewangan, et al. 2004, ApJ, L57
 Done, C. & Gierliński, M. 2004, PThPS, 155, 9
 Esin, A.A. et al. 1998, ApJ, 505, 854
 Fermi, E. 1949, PhRv, 75, 1169
 Gammie, C.F. 1998, MNRAS, 297, 929
 Goad, M.R. et al. 2005, MNRAS, accepted, astro-ph/0510185
 Haardt, F., & Maraschi, L. 1991, ApJ, 380L, 51 HM91
 Haardt, F., & Maraschi, L. 1991, ApJ, 413, 507 HM93

Haardt, F., Maraschi, L., & Ghisellini, G. 1994, ApJ, 432L, 95 1991, ApJ, 413, 507

Hirose, S. 2004, ApJ, 606, 1083,

Hubeny, I., & Hubeny, V. 1998, ApJ, 505, 558

Jenkins, L.P. et al. 2004, MNRAS, 349, 404

Jenkins, L.P. et al. 2005, MNRAS, 357, 109

King, A.R. et al. 2001, ApJ, 552L, 109

Krauss, M.I. et al. 2005, ApJ, 630, 228

Lamers, H.J.G.L.M., Cassinelli, J.P. *Introduction to Stellar Winds*, Cambridge 1999

Miller, J.M. et al. 2003, ApJ, 585L, 37

Miller, J.M. et al. 2004a, ApJ, 607, 931

Miller, J.M. et al. 2004b, ApJ, 609, 728

Miller, K.A., & Stone, J.M. 2000, ApJ, 534, 398

Miller, M.C., & Colbert, E.J.M., 2004, IJMPD, 13, 1

Miyaji, et al. 2001, AJ, 121, 3041

Narayan, R., & Yi, I. 1995, ApJ, 452, 710

Pietrini, P. & Krolik, J.H. 1995, ApJ, 447, 526

Portegies Zwart, S.F., & McMillan, S.L.W. 2002, ApJ, 576, 899

Poutanen, J., Krolik, J.H., & Ryde, F. 1997, MNRAS, 292L, 21

Quataert, E. & Gruzinov, A. 2000, ApJ, 539, 809

Rappaport, S.A., Podsiadlowski, Ph., & Pfahl, E. 2005, MNRAS, 356, 401

Riffert, H., & Herold, H. 1995, 450, 508

Robert, T.P., et al. 2005, MNRAS, 357, 1363

Ross, R.R., & Fabian, A.C. 1993, MNRAS, 261, 74

Ross, R.R., Fabian, A.C., & Young, A.J. 1999, MNRAS, 306, 461

Stern, B.E. et al. 1995, ApJ, 449, 13

Svensson, R. 1984, MNRAS, 209, 175

Svensson, R., & Zdziarski, A.A. 1994, ApJ, 436, 599

Turner, N.J. 2004, ApJ, 605L, 45

White, T.R., & Lightman, A.P. 1989, ApJ, 340, 1024

Zdziarski, A.A. 1985, ApJ, 289, 514